Proceedings of DSCC2008
2008 ASME Dynamic Systems and Control Conference
October 20-22, 2008, Ann Arbor, Michigan, USA

DSCC2008-2194

DECENTRALIZED DYNAMIC CONTROL OF A NONHOLONOMIC MOBILE MANIPULATOR COLLECTIVE: A SIMULATION STUDY

Hao Su
Mechanical & Aerospace Engineering
State University of New York at Buffalo
318 Jarvis Hall, Buffalo NY 14260 USA
E-mail: haosu@buffalo.edu

Venkat Krovi
Mechanical & Aerospace Engineering
State University of New York at Buffalo
318 Jarvis Hall, Buffalo NY 14260 USA
E-mail: vkrovi@eng.buffalo.edu

ABSTRACT

In this paper, we present a decentralized dynamic control algorithm for a robot collective consisting of multiple nonholonomic wheeled mobile manipulators (NH-WMMs) capable of cooperatively transporting a common payload. In this algorithm, the high level controller deals with motion/force control of the payload, at the same time distributes the motion/force task into individual agents by grasp description matrix. In each individual agent, the low level controller decomposes the system dynamics into decoupled task space (end-effector motions/forces) and a dynamically-consistent null-space (internal motions/forces) component. The agent level control algorithm facilitates the prioritized operational task accomplishment with the end-effector impedance-mode controller and secondary null-space control. The scalability and modularity is guaranteed upon the decentralized control architecture. Numerical simulations are performed for a 2-NH-WMM system carrying a payload (with/without uncertainty) to validate this approach.

INTRODUCTION

Cooperation is one of the key desirable characteristics of next generation robotic systems. Though much research effort is devoted to this area, less attention is paid to physically interconnected robotic systems which have many applications that make it of particular interest for study. Object transport and manipulation by cooperative multi-robot systems, like multiple planetary rovers [1] and human-supervised multiple mobile robots [2], is proved to be an effective way to handle complex and heavy payloads in unknown and dynamic environments.

However, deploying multiple robots to cooperatively manipulate common payload creates redundancy, the resolution of which has posed longstanding yet vital challenge to the robotics community. Examples of cooperative multi-robot systems, ranging from multiple mobile robots [3], multifingered hands [4], and multilegged vehicles [5] have been extensively studied in a variety of contexts. Early literature in this field addressed redundancy resolution in cooperating system from a centralized perspective. Khatib [6] studied the dynamic properties of redundant manipulators and proposed the augmented object model for multi-arm cooperation. In a later stage, Liu and Arimoto [7] addressed the adaptive control problem of multiple redundant manipulators cooperatively handling an object in a decentralized manner while optimizing a performance index. Szewczyk et al. [8] presented a distributed impedance approach for multiple robot system control which is scalable with increased robot modules. More recently, the nominal exponential stability of collaborative load transport by multiple robots is proved by Montemayor and Wen [9].

Interest has grown in mobile manipulation to achieve cooperative payload manipulation since the workspace is significantly increased. Again, while the early work mainly focused on a centralized way, such as Desai et al. [10] studied optimal motion planning for nonholonomic cooperating mobile manipulators grasping and transporting objects and Tanner et al. [11] presented a motion planning methodology for articulated, nonholonomic robots with guaranteed collision avoidance, decentralized approaches appear to show the greater potential for scalability. Similarly, while early efforts deal with holonomic mobile bases [12, 13], the attention to nonholonomic chained form system permits the ability to deploy on real world vehicles. In forming such composite systems, it is important to first ensure capability of various kinematic constraints, both at individual module and system level. Bhatt et al. [14] established a systematic framework for formulation and evaluation of system-level performance on the basis of the individual-module characteristics and affiliated kinematic constraints. A kinematically compatible framework for cooperative payload transport by nonholonomic mobile manipulators is proposed by Abou-Samah et al. [15]. Having satisfied kinematic capability, there exits the potential to further optimize the performances by

taking into account of dynamic consideration, such as interaction forces on actuation level. To facilitate the maintenance of holonomic and nonholonomic constraints within the system, dynamic controller could achieve better physical performance and improvement in the actuation input profiles.

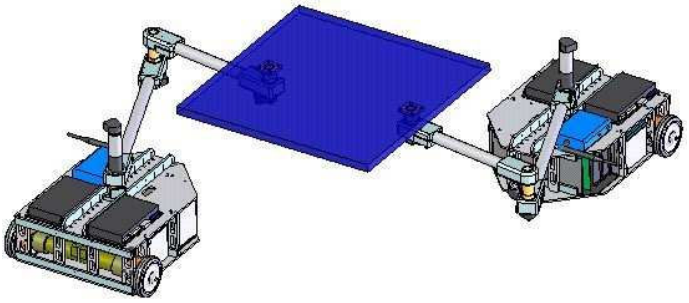

FIGURE 1: TWO ROBOT MODULES WITH A COMMON PAYLOAD

In our system, each basic module is composed of a differentially-driven wheeled mobile robot (WMR) with a mounted planar two degree-of-freedom (d.o.f) manipulator. The common payload is placed on the multiple end-effectors with passive revolute joints, as shown in Figure 1. With all of the advantages mentioned above, the entailed research challenges come from three aspects. First, the disk-like wheeled mobile bases are subjected to nonholonomic constraints, and it is well identified by Brockett [16] that nonholonomic systems as a class of systems that cannot be stabilized via smooth time-invariant state feedback law. This implies that motion planning and control of such systems deserves more special treatment. Secondly, we note that as the payload is placed on the end-effectors, it constitutes a subclass of grasp problem, so the internal forces regulation and multiple agent coordination would be of great significance for the successful implementation of this system. Finally, the increased workspaces, mobility and manipulability could be obtained in the cost of considerable redundancy which needs to be suitably resolved in a dynamic level.

By leveraging the modeling and analysis we developed in [14, 15, 17], our final goal is to establish a decentralized dynamic control framework of multiple NH-WMMs. Although the approach proposed in this paper is in a decentralized manner and applicable for multiple mobile manipulators, we would usually illustrate the cooperation scenario with two of such NH-WMMs.

Building on prior literature in the grasping content, we will treat the overall problem in a two-level hierarchical setting. The high level controller takes care of motion/force control of the payload, at the same time distributes the motion/force task into individual agents by grasp description matrix. While in each individual module, a low level controller decomposes the system dynamics into decoupled task space (end-effector motions/forces) and a dynamically-consistent null-space (internal motions/forces) component. The modular level control algorithm facilitates the prioritized operational task accomplishment with the end-effector impedance-mode controller and secondary null-space control. This allows for decentralization and further improvement in performance over the kinematic counterpart and is the main contribution of the work in this paper. The rest of the paper is organized as follows: Section 2 presents grasp modeling of the cooperative system, and the kinematic and dynamic modeling of individual NH-WMM would be addressed in Section 3. The control of individual and multiple NH-WMMs would be presented in Section 4 and 5 respectively. Finally, concluding remarks are given at the end of the paper.

MODELING OF COOPERATIVE SYSTEM

In our system, each basic module is composed of a differentially-driven WMR with a mounted planar two-d.o.f manipulator, and the schematic diagram of two cooperative robot modules is shown in Figure 2. Since our system is confined to fixture based grasping with the payload, the danger entailed by dropping of objects can always be circumvented.

We also note that the end-effector and payload level dynamics can be treated as a subclass of grasping problem. In the following analysis and modeling of NH-WMM system with payload transport, we would begin with this critical precursor to facilitate our longer-term goal of decentralized payload manipulation operations.

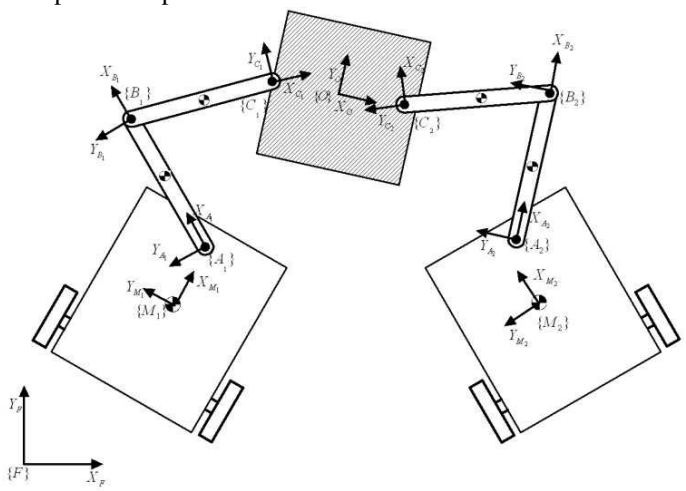

FIGURE 2: SCHEMATIC DIAGRAM OF TWO COOPERATIVE ROBOT MODULES WITH A COMMON PAYLOAD

In cooperative manipulation literature, much research effort is devoted to the internal force control. An internal force is a set of contact forces which result in no net force on the payload [18]. Internal force has usually been characterized by the null space of a matrix that relates the vector of grasp contact forces to the vector of resultant force. The first motivation of internal force control comes from the fact that large internal forces

would usually be produced in multiple manipulator motion control, thus severely deteriorate manipulated objects and energy efficiency. The other reason for characterizing and controlling internal forces is the desire to satisfy frictional constraints during multiple manipulator manipulation. Internal forces are usually defined according to the null space of the relationship between applied forces and their resultant, like the force distribution work by Kumar and Waldron [5]. Kumar et al. [19] used the characterization of grasp-force redundancy to control relative motion at the contact point, and this redundancy is used to minimize internal forces during motion. Yoshikawa [20] presented a virtual truss model for the grasped object for characterizing the internal force.

Consider N multiple manipulators rigidly grasp a common payload and each manipulator applies force/moment to the object as shown in Figure 3. For convenience, we always choose the center of mass of the payload to be the payload reference point, and we also choose the contact coordinate frame, c_i such that the z-axis of this frame points in the direction of the inward surface normal at the point of contact [18]. The world coordinate, payload coordinate and i th grasp coordinate are noted as $\{F\}$, $\{O\}$ and $\{C_i\}$ respectively. The absolute configuration of $\{O\}$ with respect to the world coordinate $\{F\}$ is given by a position vector $\underline{x}_o$ and the 3×3 rotation matrix ${}^{O}R_F$. The generalized velocity of $\{O\}$ is expressed by a 6×1 vector

$$\underline{x}_o = \begin{bmatrix} \underline{v}^T & \underline{\omega}^T \end{bmatrix}^T \tag{1}$$

where $\underline{v}$ and $\underline{\omega}$ are the linear and rotational velocity vector.

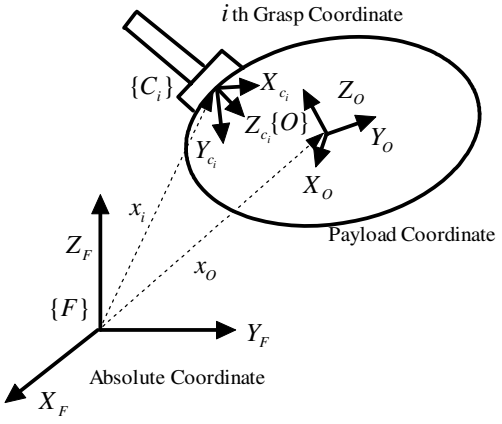

FIGURE 3: PAYLOAD GRASP NOMENCLATURE

The Newton-Euler EOMs of the payload are

$$M_o \underline{\ddot{x}}_o + \underline{C}_o = \underline{F}_o \tag{2}$$

$$M_o = \begin{bmatrix} m_o I_3 & 0_3 \\ 0_3 & I_o \end{bmatrix}, \quad C_o = \begin{bmatrix} -m_o g \\ \omega \times I_o \omega \end{bmatrix}$$

where m_o and I_o are the payload mass and inertia respectively, I_3 is the 3×3 identity matrix and 0_3 is the 3×3 null matrix. $\underline{F}_o$ is the resultant wrench vector by the multiple manipulator grasp. If we denote the wrench applied to the payload at the i th contact as $\underline{F}_i$, the cascaded vector of N forces $\underline{F} = \begin{bmatrix} \underline{F}_1^T, & \ldots & \underline{F}_N^T \end{bmatrix}^T$ would be mapped to the resultant wrench at the reference point by the $6\times6N$ grasp matrix W as

$$\underline{F}_o = W\underline{F} \tag{3}$$

Any component of the vector $\underline{F}$ that lies to the null space of W is the internal force. The null space approach works well to minimize internal forces during motion, however when the forces are regulated to a non-zero value, the resulting object deformation depends on the basis vectors used to describe the null space. So here we would adopt the virtual linkage model [21] proposed by Williams and Khatib, which is a physical characterization of internal forces. In a cooperative manipulation scheme, the relationship between applied forces and their resultant and internal forces can be described by

$$\begin{bmatrix} \underline{F}_o \\ \underline{F}_{int} \end{bmatrix} = G \begin{bmatrix} \underline{F}_1 \\ \vdots \\ \underline{F}_N \end{bmatrix} \tag{4}$$

where $\underline{F}_o$ represents the resultant forces at the reference point, $\underline{F}_{int}$ is the internal forces and $\underline{F}_i$ is the forces applied at the grasp point i. G is called the grasp description matrix, and relates the forces applied at every grasp point to the resultant and internal forces in the payload. G can be decomposed as

$$G = \begin{bmatrix} G_{res,1} & \cdots & G_{res,N} \\ G_{int,1} & \cdots & G_{int,N} \end{bmatrix} \tag{5}$$

where $G_{res,i}$ is the contribution of $\underline{F}_i$ to the resultant forces in the payload and $G_{int,i}$ to the internal ones.

The inverse relationship can be obtained as:

$$\begin{bmatrix} \underline{F}_1 \\ \vdots \\ \underline{F}_N \end{bmatrix} = G^{-1} \begin{bmatrix} \underline{F}_o \\ \underline{F}_{int} \end{bmatrix} \tag{6}$$

Similarly, the inverse of grasp description matrix, G^{-1}, can be written as

$$G^{-1} = \begin{bmatrix} \bar{G}_{res,1} & \bar{G}_{int,1} \\ \vdots & \vdots \\ \bar{G}_{res,N} & \bar{G}_{int,N} \end{bmatrix} \tag{7}$$

DECENTRALIZED CONTROL OF COOPERATIVE SYSTEM

Coordinated motion/force control of multiple serial-chain manipulators has been well studied. Here we use an object dynamics-based control algorithm to achieve a decentralized control.

If we specify the desired trajectory of the payload as $\underline{x}_o^d$, then the following resultant force

$$\underline{F}_o = \underline{C}_o + M_o(\ddot{\underline{x}}_o^d + K_{ov}(\dot{\underline{x}}_o^d - \dot{\underline{x}}_o) + K_{op}(\underline{x}_o^d - \underline{x}_o)) \qquad (8)$$

could guarantee the payload is controlled so as to satisfy the following equation

$$(\ddot{\underline{x}}_o^d - \ddot{\underline{x}}) + K_{ov}(\dot{\underline{x}}_o^d - \dot{\underline{x}}_o) + K_{op}(\underline{x}_o^d - \underline{x}_o) = 0 \qquad (9)$$

where K_{ov} and K_{op} can be tuned by pole placement.

Theoretically, from the energy consumption perspective, zero internal forces are desirable. This mechanism also implies that zero internal forces are possible to be deployed in a payload transport scheme. But practically, we still would expect to use some nonzero internal forces to guarantee the payload in some controlled equilibrium mode. With this in mind, we can determine the desired resultant forces and internal forces, and these forces would be distributed to individual agent by Eq. (6) . These distributed forces would be the desired forces for individual NH-WMM. Every NH-WMM could use the sensed local information to achieve decentralized control. The controller structure is shown in Figure 4.

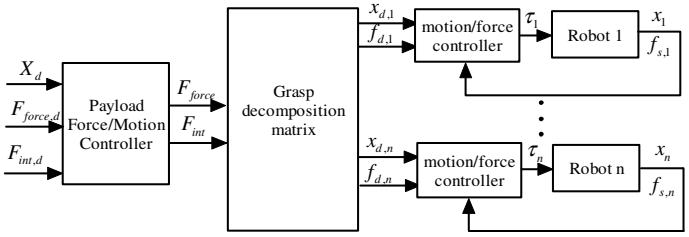

FIGURE 4: DECENTRALIZED CONTROLLER OF THE COOPERATIVE PAYLOAD TRANSPORT SYSTEM

Physically, when the payload geometry is known, the payload motion can be sensed by individual modules with the joint sensors. So one of the special features of this control structure is that this is a decentralized controller, which would be scalable with increased robot agents when more agents are necessary for some very complex task. Secondly, since for individual agent, the task/null space motion is completely decoupled with prioritized task accomplishment, the nonholonomic motion base would not affect the final end-effector performance, even when the task specified by the end-effector motion/force is conflicted with the base. This special feature would guarantee that multiple NH-WMM could always achieve good task performance while not getting conflicted with each other.

DECOUPLED TASK/NULL SPACE DYNAMIC CONTROL OF INDIVIDUAL NH-WMM [22]

In the previous section, we examined how the cooperative task can be broken down into the contribution derived from the end-effector of the individual module. In order to realize the motion/force contribution, we use a previously developed kinematic/dynamic model of a NH-WMM [23]. The salient features of the development of the controller for the redundant NH-WMM are summarized below. As shown in Figure5, each WMM is composed of a differentially-driven WMR with a mounted planar two d.o.f revolute manipulator.

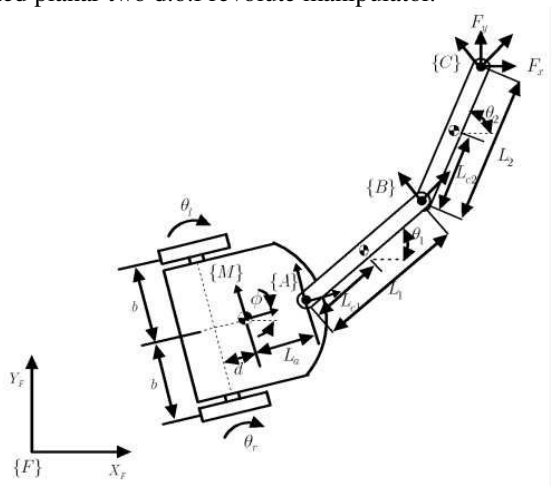

FIGURE 5: WMM NOMENCLATURE

The extended set of n generalized coordinates of the system is give by $\underline{q} = \begin{bmatrix} \underline{q}_a^T & \underline{q}_b^T \end{bmatrix}^T$. $\underline{q}_a$ are the coordinate variables describing the mobile base configuration, including the base position orientation and wheel displacement and $\underline{q}_b$ are the configuration variables of the mounted manipulator. The set of m constraints (including nonholonomic and holonomic ones) can be written in Pfaffian form as:

$$A(\underline{q})\dot{\underline{q}} = 0 \qquad (10)$$

where $A = \begin{bmatrix} -\sin\phi & \cos\phi & -d & 0 & 0 & 0 & 0 \\ -\cos\phi & -\sin\phi & -b & r & 0 & 0 & 0 \\ -\cos\phi & -\sin\phi & b & 0 & r & 0 & 0 \end{bmatrix}$.

The Euler-Lagrange dynamic equation of motion (EOM) of the constrained WMM can be described as

$$\begin{aligned} M(\underline{q})\ddot{\underline{q}} + \underline{V}(\underline{q}, \dot{\underline{q}}) &= E\underline{\tau} + E_2\underline{F} - A^T\underline{\lambda} \\ A\dot{\underline{q}} &= 0 \end{aligned} \qquad (11)$$

where $\underline{q}$ is the full set of extended generalized coordinates, including the manipulator configuration variables as mentioned above, $M(\underline{q})$ is the inertia matrix expressed in terms of the extended coordinate set, $\underline{V}(\underline{q}, \dot{\underline{q}})$ denotes the Coriolis, centrifugal

and gravity forces, E is a full rank input transformation matrix, $\underline{\tau}$ consists of the four two wheels and two arms motor inputs. $\underline{F}$ consists of the Cartesian forces applied at the end-effector. The E_2 matrix maps the task-space end-effector force, $\underline{F}$, to the joint-space. $\underline{\lambda}$ denotes the Lagrangian multiplier.

We can reformulate Eq. (11) in a partitioned manner as

$$\begin{bmatrix} M_{aa}(\underline{q}_a) & M_{ab}(\underline{q}) \\ M_{ba}(\underline{q}) & M_{bb}(\underline{q}_b) \end{bmatrix}\begin{bmatrix} \ddot{\underline{q}}_a \\ \ddot{\underline{q}}_b \end{bmatrix}+\begin{bmatrix} V_a(\underline{q},\dot{\underline{q}}) \\ V_b(\underline{q},\dot{\underline{q}}) \end{bmatrix}=\begin{bmatrix} E_a & 0 \\ 0 & E_b \end{bmatrix}\begin{bmatrix} \underline{\tau}_a \\ \underline{\tau}_b \end{bmatrix} + \begin{bmatrix} E_{2a} \\ E_{2b} \end{bmatrix}\underline{F}-\begin{bmatrix} A_a^T\underline{\lambda} \\ 0 \end{bmatrix}$$
$$A_a(\underline{q}_a)\dot{\underline{q}}_a = 0 \qquad (12)$$

where $M_{aa}(\underline{q}_a)$ is the mass matrix of the mobile based, $M_{ab}(\underline{q})$ is the inertia matrix representing the dynamic effects of the motion of the manipulator on the base, $M_{ba}(\underline{q})$ inertia matrix representing the dynamic effects of the motion of the base on the manipulator and $M_{bb}(\underline{q}_b)$ is the inertia matrix of the manipulator. $V_a(\underline{q},\dot{\underline{q}})$ and $V_b(\underline{q},\dot{\underline{q}})$ are the vectors that include Coriolis, centrifugal and gravity forces for the mobile base and manipulators respectively.

We notice that the matrix A in the Pfaffian form actually come from the mobile base, so we can also define the matrix S_a which takes the columns of S that only consists of constraints of mobile base. Thus, we can project the constrained equations on the space of feasible motions by pre-multiplying the partitioned EOM by S_a^T, and then it is simplified to

$$\left(S_a^T M_{aa} S_a\right)\ddot{\underline{z}}_a + S_a^T M_{aa}\dot{S}_a\dot{\underline{z}}_a + \left(S_a^T M_{ab} S_a\right)\ddot{\underline{q}}_b + S_a^T V_a = \underline{\tau}_a + S_a^T E_{2a}\underline{F} \qquad (13)$$

The dynamic redundancy resolution methods proposed for serial-chain redundant manipulators in [22, 24] is used with the NH-WMM. By using a weighted pseudo-inverse $\bar{J} = M^{-1}J^T\left(JM^{-1}J^T\right)^{-1}$, the control input that successfully decouples the task-space and configuration-space can then be defined [17] as:

$$\underline{\tau} = J^T W\left(\underline{u} - \dot{J}\dot{\underline{z}}\right) + \bar{N}^T M\left(\underline{v} + \dot{\bar{J}}\dot{\underline{x}}\right) + \underline{\mu}(\underline{z},\dot{\underline{z}}) + \underline{\gamma}(\underline{z}) + J^T\underline{\tau}_E \qquad (14)$$

where $W = \bar{J}^T M\bar{J}$, $\underline{\mu} = \bar{J}^T C\dot{\underline{z}} - W\dot{J}\dot{\underline{z}}$, $\underline{\gamma} = \bar{J}^T\underline{g}$. $\underline{u}$ and $\underline{v}$ are the control laws for the task-space and configuration-space, respectively.

For the task-space, we select a hybrid impedance controller [25]:

$$\underline{u} = \ddot{\underline{x}}_d + k_v\dot{\underline{e}} + k_p\underline{e} + k_f(\underline{F}_d - \underline{F}_E) \qquad (15)$$

where $\ddot{\underline{x}}_d$ is the desired acceleration; $\underline{e} = \underline{x}_d - \underline{x}$ is the position error; $\dot{\underline{e}} = \dot{\underline{x}}_d - \dot{\underline{x}}$ is the velocity error; k_v, k_p, and k_f are constants; and $\underline{F}_d$ is the desired end-effector force

For the null space controller, we use a proven dynamic tracking control method original presented by [26] and later modified for similar use in [27] that achieves input-output linearization and input-output decoupling

$$\begin{bmatrix} v_R \\ v_L \end{bmatrix} = \underline{\tau}_a = \left(S_a^T M_a S_b\right)\ddot{\underline{z}}_a + S_a^T M_{aa}\dot{S}_a\dot{\underline{z}}_a + \left(S_a^T M_{ab} S_a\right)\ddot{\underline{q}}_b + S_a^T V_a - S_a^T E_{2a}\underline{F} \qquad (16)$$

$$\ddot{\underline{z}}_a = \Phi^{-1}\left(\ddot{\underline{x}}_a - \dot{\Phi}\dot{\underline{z}}_a\right) \qquad (17)$$

$$\dot{\Phi} = \frac{d\Phi}{d\phi}c\left(\dot{\theta}_R - \dot{\theta}_L\right) \qquad (18)$$

$$\ddot{\underline{x}}_a = \ddot{\underline{x}}_a^d + k_{av}\left(\dot{\underline{x}}_a^d - \dot{\underline{x}}_a\right) + k_{ap}\left(\underline{x}_a^d - \underline{x}_a\right) \qquad (19)$$

SIMULATION RESULTS

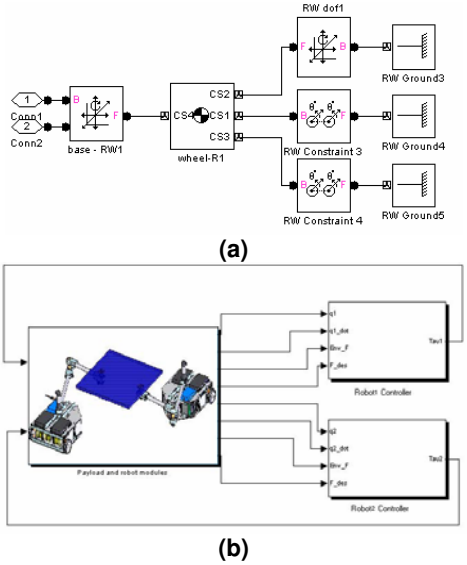

FIGURE 6: SIMMECHANICS MODEL :(A) A NONHOLONOMIC WHEEL; (B) THE SIMULATION ARCHITECTURE IN SIMULINK

In the first stage, we employ SimMechanics and SIMULINK to rapidly create, evaluate and refine parametric models of the overall system and test various algorithms within a simulation environment. A simplified solid model of the mobile platforms and the manipulators of interest is created in a SolidWorks, and exported with the corresponding geometric and material properties into SimMechanics. The controller is implemented in SIMULINK and the payload model and the

NH-WMM model is build with SimMechanics. The nonholonomic model in SimMechanics is set up with the in-build velocity constraint block as shown in Figure 6(a) and the overall simulation architecture is shown in Figure 6(b). All the parameters of the mobile manipulator are shown in Table 1.

TABLE 1: MOBILE MANIPULATOR PARAMETERS

Parameters	Values	Units
Mass of the wheel	0.159	kg
Mass of mobile base	17.25	kg
Mass of Link 1	2.56	kg
Mass of Link 2	1.07	kg
Moment of inertia of the wheels about its center of mass (CM)	2.00×10^{-4}	kg-m^2
Moment of inertia of mobile base about its CM	0.297	kg-m^2
Moment of inertia of Link 1 about its CM	0.148	kg-m^2
Moment of inertia of Link 2 about its CM	0.0228	kg-m^2
Radii of the wheels	0.0508	m
Distance from the center of the wheel axle to the CM of the mobile base	0.116	m
Distance from CM of the mobile base to the point P_a	0.100	m
Length of Link 1	0.514	m
Length of Link 2	0.362	m
Payload length	0.4	m

Case Study I: Without Uncertainty

We test the null-space controller with dynamic path-following along with the end-effector impedance-mode controller. Figure 7 shows the results from testing performed with a primary controller implementing a task-space impedance-mode for the end-effector and a secondary dynamic path-following controller for the WMR base. Here, the payload is 2kg and is commanded to tracking a sinusoid curve with $\underline{r}^d = \left[0.5+0.1t \quad 0.25\sin(0.2\pi t)\right]^T$.

To facilitate the motion planning, we specify a priori designed end-effector trajectory and mobile platform for the individual robot. If we note the length of the payload as l, the desired end-effector trajectory and motion base trajectory for the first NH-WMM are:

$$\underline{r}_{EE1}^d = \left[0.5+0.1t \quad 0.25\sin(0.2\pi t)+0.5l\right]^T$$

$$\underline{r}_{base1}^d = \left[0.1t \quad 0.3+0.5l\right]^T$$

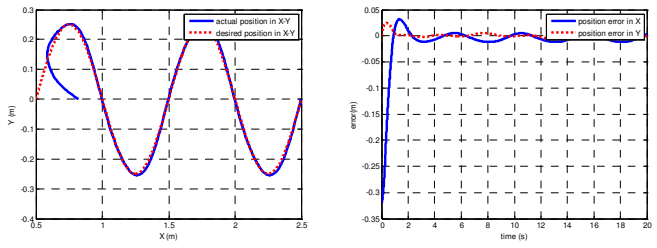

(A) (B)

FIGURE 7. PAYLOAD MOTION PROFILE. (A) DESIRED AND ACTUAL PAYLOAD TRAJECTORY, (B) X & Y TRACKING ERROR

And the desired end-effector trajectory for the second NH-WMM is:

$$\underline{r}_{EE2}^d = \left[0.5+0.1t \quad 0.25\sin(0.2\pi t)-\frac{l}{2}\right]^T$$

$$\underline{r}_{base2}^d = \left[0.1t \quad -0.3-\frac{l}{2}\right]^T$$

Since we only care about the translational motion of the payload, these two end-effector trajectories are kinematically consistent. It is necessary to note that since the grasp description matrix incorporates the resultant moment term, the payload rotational position can also be achieved in a similar manner.

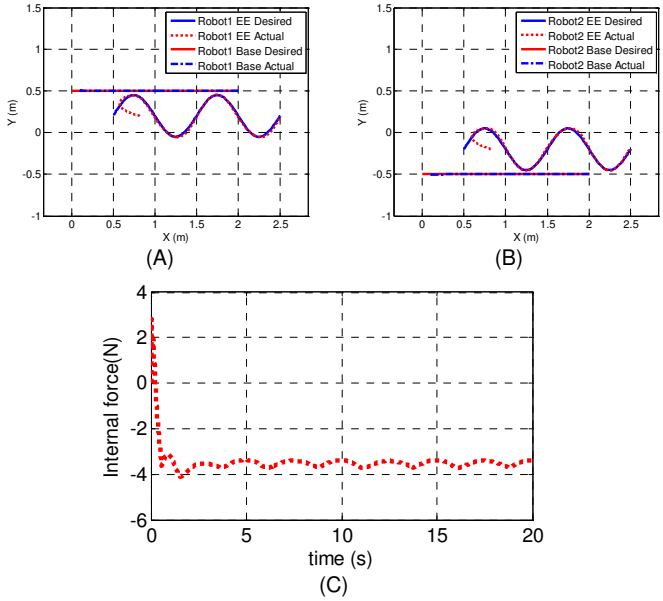

FIGURE 8. THE MOBILE PLATFORM TRACKING A LINE AND END-EFFECTOR TRACKING A SINUSOID CURVE. (A) BASE AND END-EFFECTOR TRACKING RESULTS FOR ROBOT1, (B) BASE AND END-EFFECTOR TRACKING RESULTS FOR ROBOT2, (C) INTERNAL FORCE

Figure 7 (a) is the tracking performance of the payload in Cartesian space. Figure 7 (b) shows the tracking error in Cartesian space with respect to time. The payload is enforced to track the desired trajectory with the motion controller and initial deviation would decrease within 2 seconds. The controller is capable of correcting the initial error and enforcing good tracking profiles. Figure 8 shows the tracking performance of individual agent. Figure 8(a) shows the end-effector and base tracking results for robot 1. And the same performance for robot 2 is shown in Figure 8(b). All the trajectories are converged to the desired position within 4 seconds. But we also note that since the end-effector is asked to maintain some desired forces, this would result in some minor position error in the task space.

Figure 8(c) is the internal force profile of the grasped payload. We can see that after some initial oscillation, the internal force is regulated to the value around the desired ones.

Case Study II: With Mass Uncertainty

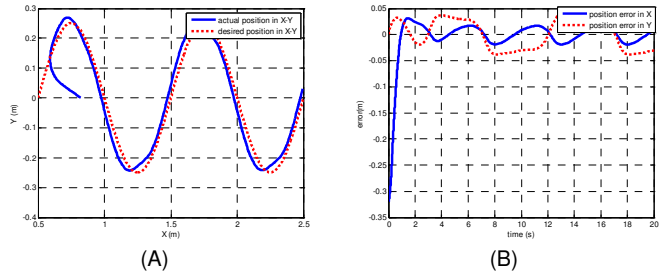

FIGURE 9. PAYLOAD MOTION WITH MASS UNCERTAINTY. (A) DESIRED & ACTUAL PAYLOAD TRAJECTORY, (B) TRACKING ERROR IN X AND Y

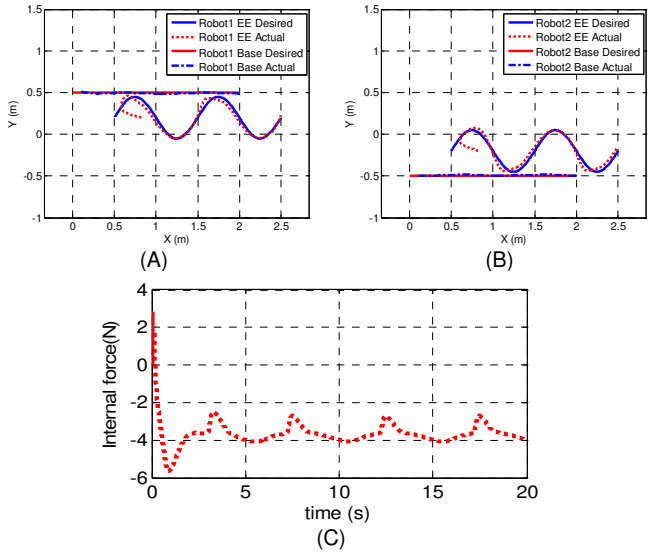

FIGURE 10. THE MOBILE PLATFORM TRACKING A LINE AND END-EFFECTOR TRACKING A SINUSOID CURVE WITH MASS UNCERTAINTY. (A) BASE TRACKING ERROR FOR ROBOT1, (B) END-EFFECTOR TRACKING ERROR FOR ROBOT1, (C) INTERNAL FORCE

In a practical robot working scenario, the parameters of robotic system or working environment are always varying. In this case study, we consider the payload mass uncertainty (which is frequently encountered in real world application) in order to study the robustness and sensitivity of the controller to uncertainty. In this case study, we underestimate the payload mass to be 1.5kg (recall that the actual payload is 2 kg). Figure 9 (a) shows the tracking performance of the payload in Cartesian space. Figure 9(b) shows the time history of Cartesian tracking error. While reflecting the degeneration in performance, due to poor estimation of the mass, the results remain nevertheless bounded. Correspondingly, Figure 10 shows the tracking performance of individual agent with mass uncertainty. Figure 10(a) and Figure 10(b) show the end-effector and base tracking results for robot 1 and 2. Figure 10(c) is the profile of the internal force in the grasped payload, wherein larger oscillation can be observed.

DISCUSSION

The coupling of the nonholonomic base constraints and the significant inherent redundancy in NH-WMMs create significant challenges for control of end-effector (motion/force) interactions. The focus of this paper is to set up a decentralized motion/force control structure for payload transport by taking advantage of a dynamic-level redundancy-resolution strategy for NH-WMMs. For individual agent, the primary task was assumed to be one of controlling the motion and/or force interactions of the end-effector with respect to the attached payload/external environment. Once the primary end-effector task has been accomplished, the secondary task is assumed to be one of controlling the surplus degrees-of-freedom within the system (relative pose of the mobile base).

The unique features of this control strategy come from three aspects. First, the payload controller is independent from the NH-WMM controller, and this implies that any established rigid body control algorithm (like sliding mode control, model reference adaptive control) can be deployed for the payload control while not affecting the NH-WMM control architecture. Specifically, in case study II, it would be possible to design a payload mass adaptive controller to observe the mass uncertainty. Second, since the individual NH-WMM controller decouples the task-space and null-space motion, multiple nonholonomic constraints would not be a problem in this cooperative schemes. And all the task-space performance would be always prioritized and guaranteed. Finally, this control architecture permits individual agent to perform formation if the formation geometry is compatible with the corresponding end-effector motion. Though the obstacle avoidance problem is not studied here, some well-developed formation control algorithm with collision avoidance, like [28], possibly could be applied to the mobile base for this purpose. This research is still under development.

ACKNOWLEDGMENT

We gratefully acknowledge the support from National Science Foundation CAREER Award (IIS-0347653) for this research effort.

REFERENCES

[1] Huntsberger, T. L., Trebi-Ollennu, A., Aghazarian, H., Schenker, P. S., Pirjanian, P., and Nayar, H. D., 2004, "Distributed control of multi-robot systems engaged in tightly coupled tasks," Autonomous Robots, **17**(1), pp. 79-92.

[2] Nakamura, A., Ota, J., and Arai, T., 2002, "Human-supervised multiple mobile robot system," IEEE Transactions on Robotics and Automation, **18**(5), pp. 728-43.

[3] Cao, Y. U., Fukunaga, A. S., Kahng, A. B., and Meng, F., 1995, "Cooperative mobile robotics: Antecedents and directions," Pittsburgh, PA, USA.
[4] Salisbury, J. K. and Craig, J. J., 1981, "Articulated hands: force control and kinematic issues," Charlottesville, VA, USA.
[5] Kumar, V. and Waldron, K. J., 1988, "Force distribution in closed kinematic chains," Philadelphia, PA, USA.
[6] Khatib, O., 1995, "Inertial properties in robotic manipulation. An object-level framework," International Journal of Robotics Research, **14**(1), pp. 19-36.
[7] Liu, Y.-H. and Arimoto, S., 1998, "Decentralized adaptive and nonadaptive position/force controllers for redundant manipulators in cooperations," International Journal of Robotics Research, **17**(3), pp. 232-47.
[8] Szewczyk, J., Plumet, F., and Bidaud, P., 2002, "Planning and controlling cooperating robots through distributed impedance," Journal of Robotic Systems, **19**(6), pp. 283-97.
[9] Montemayor, G. and Wen, J. T., 2005, "Decentralized collaborative load transport by multiple robots," Barcelona, Spain.
[10] Desai, J. P. and Kumar, V., 1999, "Motion planning for cooperating mobile manipulators," Journal of Robotic Systems, **16**(10), pp. 557-79.
[11] Tanner, H. G., Loizou, S. G., and Kyriakopoulos, K. J., 2003, "Nonholonomic navigation and control of cooperating mobile manipulators," IEEE Transactions on Robotics and Automation, **19**(1), pp. 53-64.
[12] Khatib, O., Yokoi, K., Chang, K., Ruspini, D., Holmberg, R., and Casal, A., 1996, "Coordination and decentralized cooperation of multiple mobile manipulators," Journal of Robotic Systems, **13**(11), pp. 755-64.
[13] Tan, J. and Xi, N., 2003, "Integrated Task Planning and Control for Mobile Manipulators," International Journal of Robotics Research, **22**(5), pp. 337-354
[14] Bhatt, R., Tang, C. P., Abou-Samah, M., and Krovi, V., 2005, "A screw-theoretic analysis framework for payload manipulation by mobile manipulator collectives," Orlando, FL, United States.
[15] Abou-Samah, M., Tang, C. P., and Krovi, R. M. B. V., 2006, "A kinematically compatible framework for cooperative payload transport by nonholonomic mobile manipulators," Autonomous Robots, **21**(3), pp. 227-242.
[16] Brockett, R. W., 1983, "Asymptotic Stability and Feedback Stabilization," in *Differential Geometric Control Theory*, R. W. Brockett, R. S. M. and Sussmann, a. H. J., Eds.: Boston, MA: Birkhauser, pp. 181-191.
[17] White, G. D., Bhatt, R. M., and Krovi, V. N., 2007, "Dynamic redundancy resolution in a nonholonomic wheeled mobile manipulator," Robotica, **25**147-56.
[18] Murray, R., Li, Z., and Sastry, S., 1994 *A Mathematical Introduction to Robotic Manipulation*. CRC Press,
[19] Kumar, V., Yun, X., Paljug, E., and Sarkar, N., 1991, "Control of contact conditions for manipulation with multiple robotic systems," Sacramento, CA, USA.
[20] Yoshikawa, T., 1999, "Virtual truss model for characterization of internal forces for multiple finger grasps," IEEE Transactions on Robotics and Automation, **15**(5), pp. 941-947.
[21] Williams, D. and Khatib, O., 1993, "The virtual linkage: a model for internal forces in multi-grasp manipulation," Atlanta, GA, USA.
[22] Nemec, B. and Zlajpah, L., 2002, "Force Control of Redundant Robots in Unstructured Environment," Industrial Electronics, IEEE Transactions on, **49**(1), pp. 233-240.
[23] White, G., 2006, "Simultaneous Motion and Interaction Force Control of a Nonholonomic Mobile Manipulator," Master thesis thesis, SUNY at Buffalo, Buffalo, NY.
[24] Khatib, O., 1987, "A unified approach for motion and force control of robot manipulators: the operational space formulation," IEEE Journal of Robotics and Automation, **RA-3**(1), pp. 43-53.
[25] Anderson, R. and Spong, M., 1988, "Hybrid impedance control of robotic manipulation," IEEE Journal of Robotics and Automation **4**(5), pp. 549-556
[26] Sarkar, N., Xiaoping, Y., Vijay, K., 1994, "Control of Mechanical Systems With Rolling Constraints: Application to Dynamic Control of Mobile Robots," International Journal of Robotic Research, **13**(1), pp. 55-69.
[27] Bhatt, R., 2007, "Towards Modular Cooperation between Multiple Nonholonomic Mobile Manipulators," PhD Thesis thesis, SUNY at Buffalo, Buffalo, NY.
[28] Mastellone, S., Stipanovic, D. M., Graunke, C. R., Intlekofer, K. A., and Spong, M. W., 2008, "Formation control and collision avoidance for multi-agent non-holonomic systems: Theory and experiments," International Journal of Robotics Research, **27**(1), pp. 107-126.